Optical Materials 99 (2020) 109598

Contents lists available at ScienceDirect

Optical Materials

journal homepage: http://www.elsevier.com/locate/optmat

Heterojunction bipolar light-emitting transistors (HBLETs) fabricated with a lateral emission geometry for real-time optical wireless transmission

Chia-Lung Tsai [a,b,*], Yi-Chen Lu [a], Chih-Min Yu [a], Chia-Yu Yu [a], Sun-Chien Ko [c], Meng-Chyi Wu [d]

[a] Department of Electronic Engineering and Green Technology Research Center, Chang Gung University, Taoyuan, Taiwan
[b] Department of Otolaryngology-Head and Neck Surgery, Chang Gung Memorial Hospital, Taoyuan, Taiwan
[c] Advanced Tech. Research Lab., Telecommunication Lab., Chunghwa Telecom Co., Ltd., Taoyuan, Taiwan
[d] Institute of Electronics Engineering, National Tsing Hua University, Hsinchu, Taiwan

ARTICLE INFO

Keywords:
HBLETs
Lateral emission geometry
Optical wireless communications

ABSTRACT

Heterojunction bipolar light-emitting transistors (HBLETs) with a cleaved facet in the lateral direction for light emission are proposed for real-time optical wireless transmission. To prevent light shielding by the top metal electrodes, the light output power of the edge-emitting HBLETs exceeds that of those emitting from the top surface. Although the proposed HBLETs can generate spontaneous light emissions at $\lambda \sim 965$ nm, a reduced common-emitter current gain ($\beta \sim 0.41$) was found due to some of the minority carriers (electron) from the emitter being radiatively recombined within the $In_{0.15}Ga_{0.85}As/GaAs$ multiple-quantum-well containing base layer. Results also show that a 300 Mbit/s optical link can be constructed using the proposed HBLET transmitter with a lateral emission geometry but its modulation bandwidth is as high as 237.5 MHz. The paper also describes the use of HBLET-based optical wireless communications to achieve real-time transmissions of digital TV signals over a distance of 100 cm in free space.

1. Introduction

Optical wireless communications possess several promising features such as high data transmission rates and reduced power and mass deployment requirements. These techniques are increasingly critical for relieving the continuously expanding data volume in conventional radio-frequency (RF)-based links (e.g., Wi-Fi) [1]. Compared with other optical wireless links, light-emitting diode (LED)-based optical wireless links offer benefits of license-free and unregulated bandwidth in the visible to near-infrared wavelengths, immunity to electromagnetic interference, network security and low system cost, making they more suitable for co-use with Wi-Fi in Internet of Things (IoT) applications or 5G networks [2,3]. However, LED transmitters suffer from a slow dynamic response due to their parasitic resistance–capacitance elements or nonoptimized epistructure design (which causes increased carrier lifetime), which will significantly restrict the transmission performance of such optical links. By shrinking the device size to a few 10-μm, an orthogonal frequency division multiplexing (OFDM)-based bi-directional optical link with respective downlink and uplink data rates of 416 Mbps and 165 Mbps has been proposed using an integrated optical transceiver composed of a transfer printed micro-LED transmitter on the fluorescent concentrator and an avalanche photodiode (APD) [4]. Using a strain-compensation scheme to control the polarization field of InGaN LEDs, the decrease in carrier lifetime reflects an increased speed of up to 117 MHz for blue InGaN/GaN LEDs under 0.14% compressive strain [5]. Shen et al. reported that the presence of amplified spontaneous emissions in 405 nm superluminescent diodes (SLDs) grown on a semipolar GaN substrate helps increase light output power and 3-dB modulation bandwidth ($f_{3dB} = 807$ MHz) [6]. In addition, an SLD-based on-off keying optical link can transmit data at a rate of 622 Mbps with a bit-error rate of 4×10^{-4}.

By using a reversely biased base-collector junction as an electron collector while placing an InGaAs/GaAs multiple-quantum-well (MQW) in a thin and highly carbon-doped ($>10^{19}$ cm^{-3}) base layer to facilitate effective light emission, novel optoelectronic devices of *n-p-n* heterojunction bipolar light-emitting transistors (HBLETs) have been proven to be useful for high-speed optical data transmission [7]. However, such devices have yet to be shown to function as optical transmitters in the aforementioned optical wireless links. This study experimentally investigates the feasibility of an optical wireless link using HBLETs. The lateral emission design prevents emission light from being blocked by the top metal electrodes, resulting in improved light output power of the

* Corresponding author. Department of Electronic Engineering and Green Technology Research Center, Chang Gung University, Taoyuan, Taiwan.
E-mail address: cltsai@mail.cgu.edu.tw (C.-L. Tsai).

https://doi.org/10.1016/j.optmat.2019.109598
Received 14 October 2019; Received in revised form 29 November 2019; Accepted 2 December 2019
Available online 9 December 2019

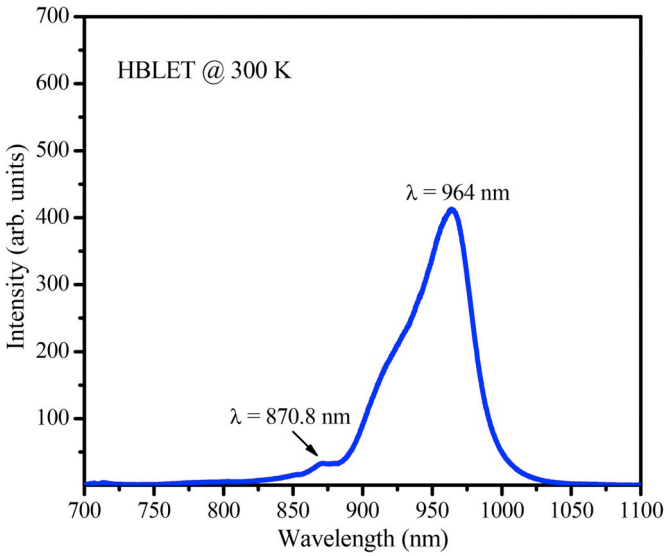

Fig. 1. PL spectrum of the HBLET wafer without the topmost GaAs layer.

fabricated HBLETs. In addition, these transistor outline (TO)-can packaged HBLETs not only exhibit a high modulation bandwidth of 237.5 MHz but are also suitable for use in directed line-of-sight optical links for real-time data transmissions.

2. Experimental

The epistructure of *n-p-n* HBLETs used here was grown on a semi-insulating GaAs substrate and consists of a GaAs buffer layer, a heavily Si-doped ($>10^{19}$ cm^{-3}) GaAs subcollector, an $In_{0.49}Ga_{0.51}P$ etch stop layer and a lightly Si-doped (1×10^{16} cm^{-3}) GaAs collector. These layers are followed by the p-base layer (total thickness of ~106 nm) in which two pairs of undoped-$In_{0.15}Ga_{0.85}As$ (11.2 nm)/GaAs (carbon doping ~ 3×10^{19} cm^{-3}, 17.9 nm) MQWs were grown for light emitting at λ ~ 960 nm. To reduce the extent of conduction band discontinuity between the $In_{0.49}Ga_{0.51}P$ emitter and the p-base layer, a p-$Al_{0.1}Ga_{0.9}As$ interfacial layer was introduced [8]. The growth procedure was terminated with the Si-doped ($>10^{19}$ cm^{-3}) GaAs contact layer. Fig. 1 shows the photoluminescence (PL) spectrum (532 nm excitation) of the HBLET wafer without the topmost GaAs layer. The dominant PL peak at λ = 964 nm is correlated to the $In_{0.15}Ga_{0.85}As$/GaAs MQWs buried in the base layer [7]. As a result of P and As intermixing at the InGaP/(Al)GaAs interface during epitaxial growth [9], an additional peak (λ ~ 871 nm)

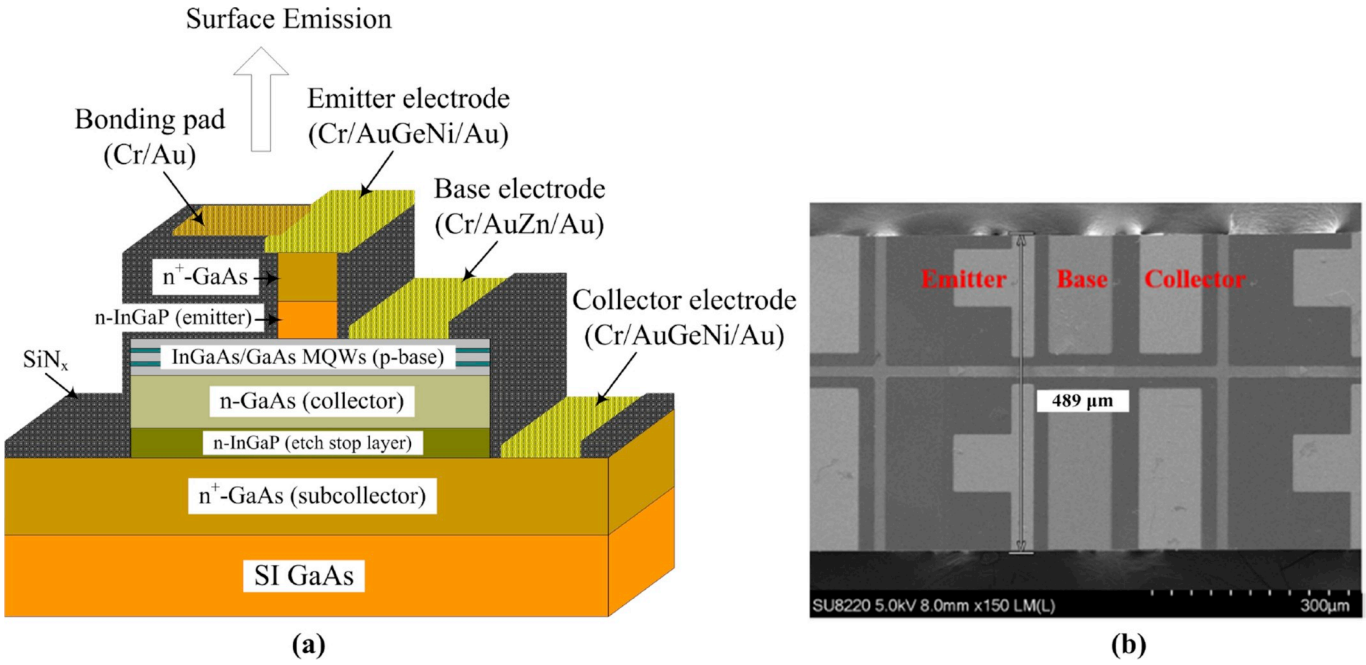

Fig. 2. (a) Schematic diagram of *n-p-n* HBLETs incorporated with two InGaAs/GaAs MQWs buried in the base layer for light emission, and (b) the corresponding top-view SEM image of the completed HBLETs with edge emission geometry. The emitter area of the HBLET is estimated at 24 × 490 μm^2.

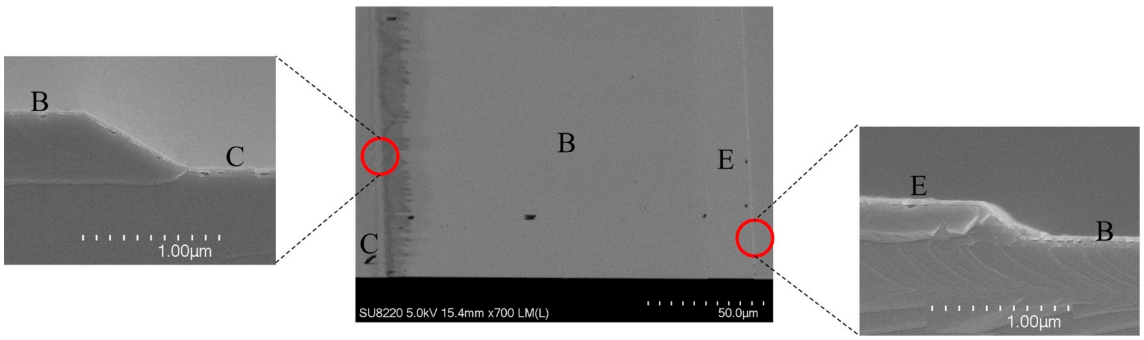

Fig. 3. The cross-sectional SEM image of the HBLET wafer after the mesa formation process.

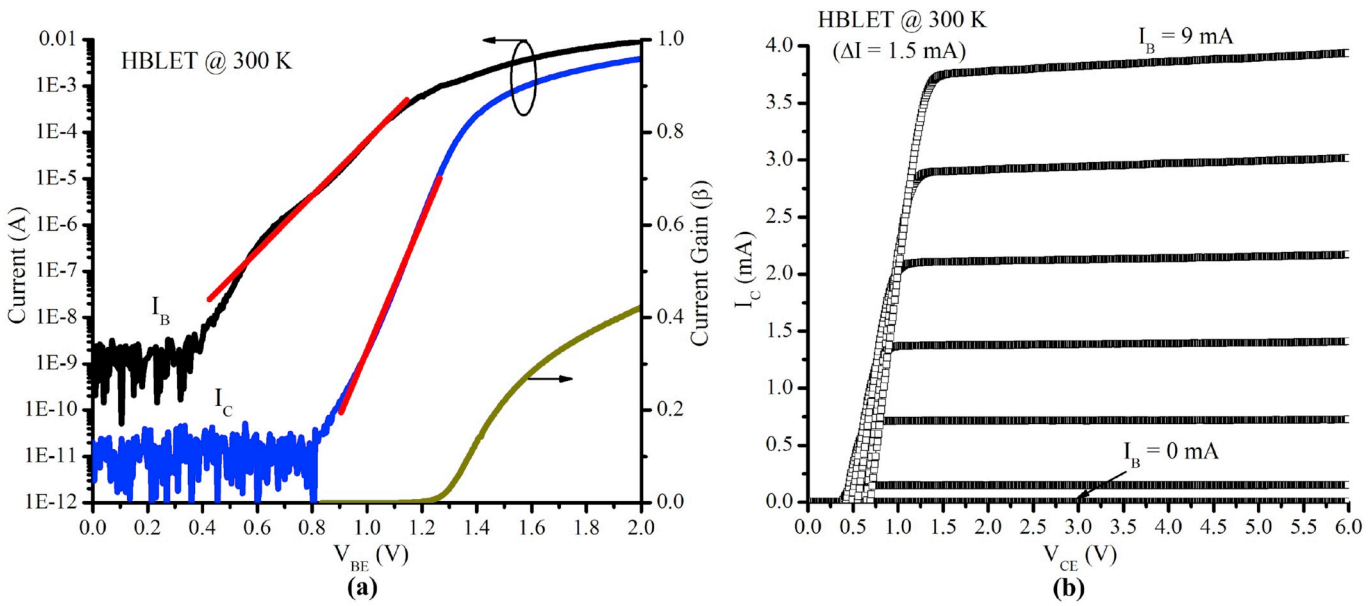

Fig. 4. (a) Gummel plot of I_C and I_B for the fabricated HBLETs with zero bias at the base-collector junction. The dependency of the current gain ($\beta = I_C/I_B$) on different V_{BE} is also shown in the figure. (b) Common emitter I–V characteristics of these devices.

associated with the light emission from the InGaAsP layer can also be observed in this figure. The production process of the HBLETs with a lateral emission geometry is similar to previous reports [7], where the main process is the formation of a step-shaped mesa [Fig. 2(a)] by wet etching to allow for subsequent production of the strip-shaped n-emitter along with the metal contact regions of the p(n)-base (collector). Fig. 3 shows the cross-sectional scanning electron microscopy (SEM) image of the HBLET wafer following the mesa formation process. The step height of the emitter mesa is evaluated as ~251 nm, while a 400-nm-height base mesa was formed on the collector. Prior to metallization, the whole wafer surface was passivated with SiN_x for electrical insulation between the emitter and the base. Wafer thinning/cleaving was

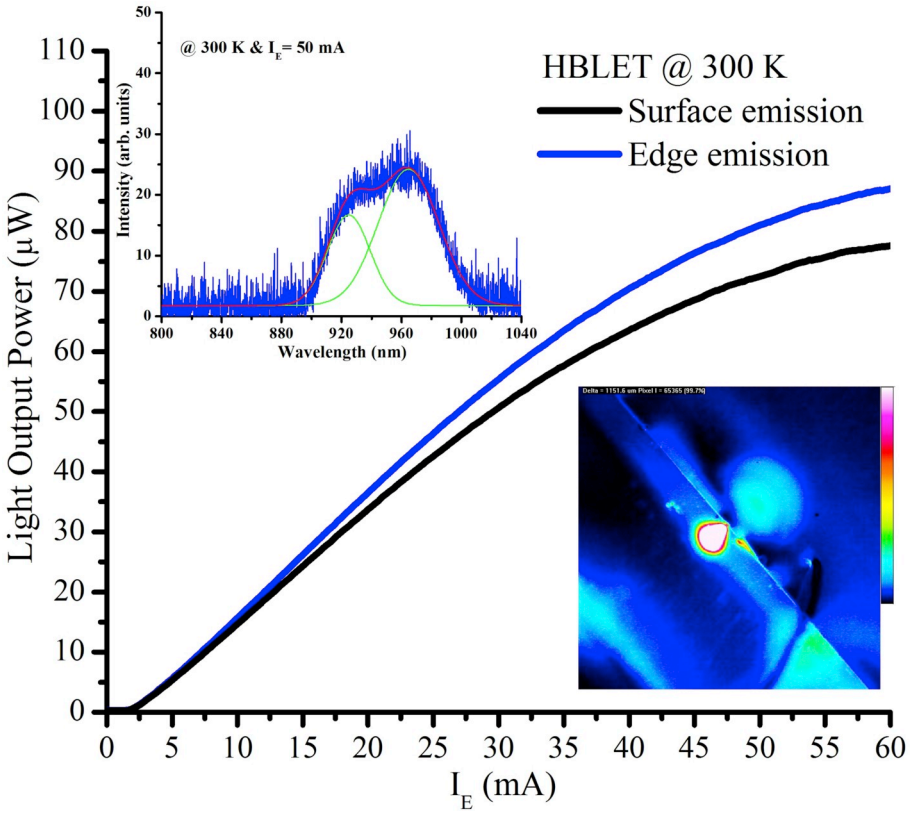

Fig. 5. L-I_E characteristic curves at 300 K measured from the vertical or lateral direction of the HBLETs operated with $V_{BC} = 0$ V and $V_{BE} > 0$. The inset shows the EL spectrum and the near-field emission pattern of the edge-emitting HBLET measured at $I_E = 50$ mA. Two constituent components at $\lambda = 965$ and 925 nm can be achieved through Gaussian fitting of the measured spectral data.

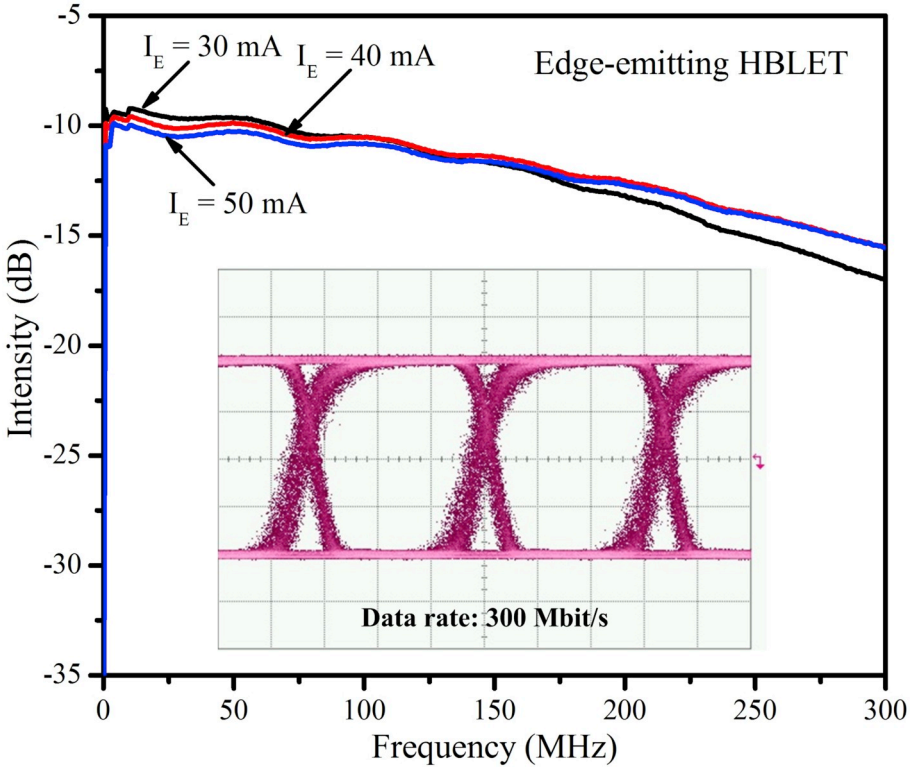

Fig. 6. Dynamic response of the edge-emitting HBLET operated with $V_{BC} = 0$ V and $I_E > 0$. The inset shows the eye diagram measured at 300 Mbit/s with $I_{Bias} = 50$ mA, $V_{PP} = 5$ V and PRBS = 2^7-1. For both measurements, the used optical link is identical to that shown in Fig. 7(a).

followed by the production of the edge-emitting HBLET with a strip-shaped emitter (area ~24 × 490 μm^2), as shown in Fig. 2(b). To characterize the current-voltage (I–V) curves by Agilent 4155B semiconductor parameter analyzer, the light output performance of the completed HBLETs without packaging was measured using a Keithley Model 2400 source meter and a calibrated integrating optical sphere sensor (Newport Corp.). For high-frequency testing, the HBLET chips were first packaged onto a TO-56 header without encapsulation and were then soldered with a coaxial 50 Ω SMA microwave connector through a printed circuit board.

3. Results and discussion

Fig. 4(a) shows the Gummel plot of the collector current (I_C) and base current (I_B) for the HBLETs with zero base-collector voltage ($V_{BC} = 0$ V). At 300 K, the HBLET exhibits a slightly high turn-on voltage ($V_{BE,ON}$) of 1.35 V as the collector current per unit emitter area (J_C) approaches 1 A/cm^2. In addition, the collector (base) current ideality factor [$n_{C(B)}$] of the HBLETs from the slope of the semi-logarithmic I–V characteristics are respectively estimated at 1.2 and 2.8. The low value of n_C is considered a result of the diffusion-driven current in the base layer due to the electrons injected from the emitter to the collector crossing over the base through the diffusion process. Because the extrinsic base region of the fabricated HBLETs is only coated with an insulating dielectric (SiN_x), the unoptimized surface passiviation [10], together with the space-charge recombination at the base-emitter junction [11], will cause increased carrier leakage and produce the higher n_B (>2) found in these devices. As evaluated from the common emitter I–V characteristics [Fig. 4(b)], the HBLETs have a 0.44 V offset voltage and the achievable current gain ($\beta = I_C/I_B$) is about 0.41 at $I_B = 9$ mA. The variation of the current gain with different V_{BE} can also be found in Fig. 4(a). Although the proposed HBLETs can generate photons (as shown in Fig. 5), the original collector current will now be partly shared to the radiative recombination current due to the injected carriers (electrons) being partly annihilated within the InGaAs/GaAs MQWs of the base layer. This is responsible for their low current gain or increased turn-on voltage as compared to those of conventional HBTs [12].

Fig. 5 shows the light output power-emitter current (L-I_E) characteristic curves at 300 K measured from the vertical or lateral direction of the HBLETs operated with $V_{BC} = 0$ V and $V_{BE} > 0$. Although the base and collector of the HBLETs under test is set as equipotential, the presence of a non-negligible voltage drop in the base spreading resistance helps the base-collector junction to stay in reversely biased condition and thus reduce the recovery time of the transistor [13]. As shown in Fig. 5, a 12.2% (@ $I_E = 60$ mA) increase in light output power is achieved as the integrating optical sphere sensor is placed laterally to the HBLETs for light collection. As shown in Fig. 2(b), the emission area of light collected from the top surface of the HBLETs is evaluated as ~ 110 × 490 μm^2 by using a CCD camera (DataRay, WinCamD-UCD23). In these regions (located on both sides of the n-emitter mesa), the light intensity is significantly weaker than that obtained from the n-emitter mesa provided it is not covered by a metal layer. However, more uniform and intense emission patterns are observed from the lateral direction of the HBLETs, as shown in Fig. 5. Therefore, the improvement in light intensity of the edge-emitting HBLETs could be attributed to the relief of the light shielding from the emitter (base) metal electrodes. As shown in the inset of Fig. 5, two constituent components (located at λ = 965 and 925 nm) can be well resolved from the emission spectrum of the edge-emitting HBLET, which are respectively attributed to light emission from the $In_{0.15}Ga_{0.85}As$/GaAs MQW [7] and the p-type GaAs base [14]. In addition, the broader emission linewidth at λ = 965 nm (Δλ ~ 40 nm) suggests that the light generated from the HBLETs is mostly dominated by the spontaneous emission process.

With the lateral emission design, the fabricated HBLETs not only exhibit enhanced light output power but can also simultaneously perform output power monitoring by detecting the light emission from the opposite facet, making the edge-emitting HBLETs useful for optical data transmission. Therefore, the feasibility of using these devices as an

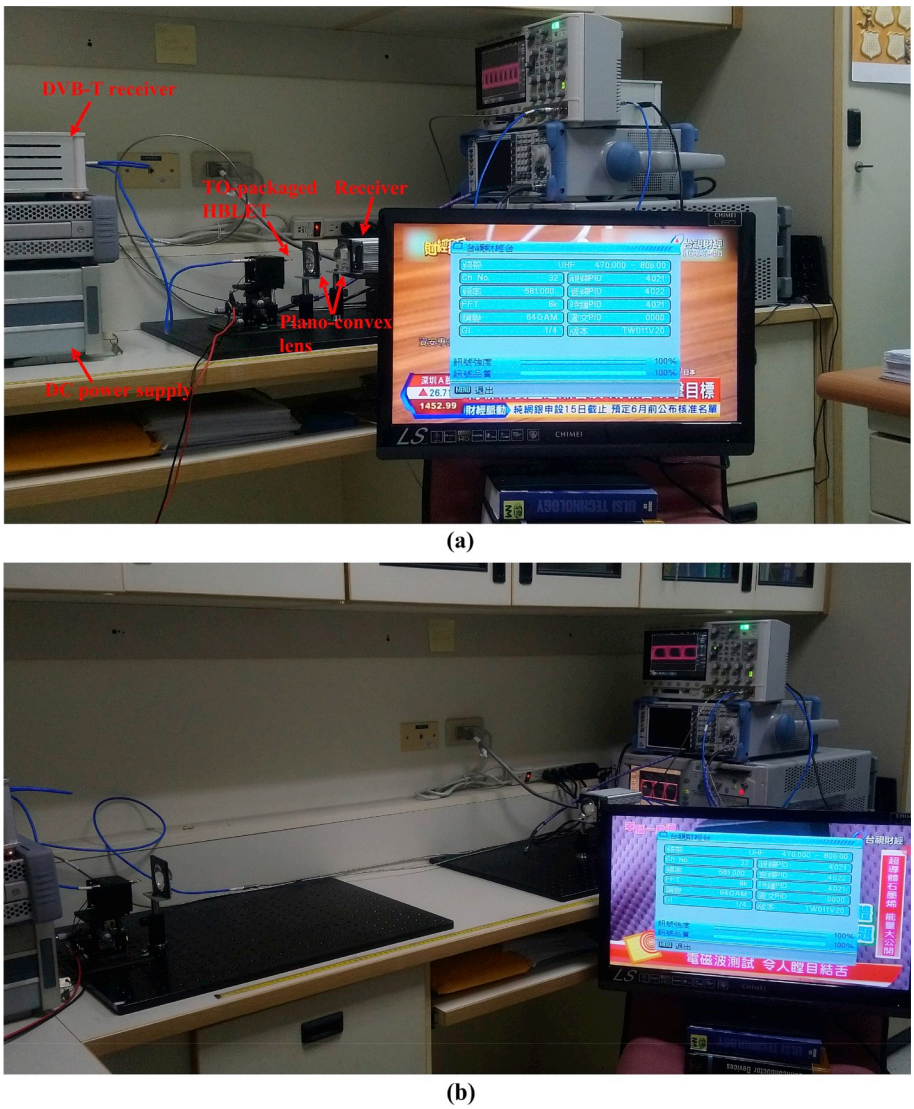

Fig. 7. Experimental setup of HBLET-based optical wireless link used for real-time transmissions of the digital video broadcasting-terrestrial (DVB-T) signals. Real-time TV signals (video only) can be clearly observed on the monitor even when the distance between the transmitter and the receiver was increased from (a) 10 cm to (b) 100 cm.

optical transmitter is experimentally investigated. Fig. 6 shows the dynamic response of the edge-emitting HBLET operated with $V_{BC} = 0$ V and $I_E > 0$. The experimental setup for the dynamic characterization is mainly composed of an optical transmitter (TO-56 packaged HBLET), an optical receiver (Pacific AD500-9-400M-TO5) and a Rohde & Schwarz ZVL network analyzer, as shown in Fig. 7(a). Using two plano-convex lenses (Edmund Optics, 40.0 mm Dia. x 60.0 mm FL uncoated plano-convex lens) with convex surfaces facing each other for light coupling between the optical transmitter and the receiver [15], a coupling efficiency of 40.6% can be achieved at a light propagation distance of 10 cm. As shown in Fig. 6, the 3-dB modulation bandwidth of the edge-emitting HBLET increased from 168.3 to 237.5 MHz as the DC bias current ($I_{Bias} = I_E$) increased from 30 to 50 mA. LED modulation bandwidth is inversely proportional to the differential carrier lifetime [16]. The increased bandwidth of the HBLET with increasing current implies enhanced spontaneous emission rate or reduced radiative lifetime of carriers within the InGaAs/GaAs MQWs of the base layer, provided that the nonradiative lifetime is fixed for the device under test. Although the presence of tilted-charge distribution of the minority carriers in the MQW containing p-base with high doping density ($>10^{19}$ cm^{-3}) helps the proposed edge-emitting HBLETs operate at high speeds, the achievable bandwidth is still lower than that of tilted-charge LEDs [17]. As shown in Fig. 2(a), the metal contact electrodes of the HBLETs are designed with a large area ($>90 \times 90$ μm^2) for electrical connection (wire bonding) of the emitter and base to the I/O terminals of TO-56 metal-can package. The extrinsic parasitic resistance–capacitance delay time associated with carrier transport at lateral p-base layer (located on both sides of the n-emitter mesa) is considered to be detrimental to the high frequency performance of the fabricated HBLETs [18]. However, as evaluated from the large-signal analysis of the edge-emitting HBLETs operated at a 50-mA bias current and a 5 V peak-to-peak voltage (V_{pp}), a clear open eye pattern is measured at 300 Mbit/s with a 2^7-1 nonreturn-to-zero pseudorandom bit sequence (see inset of Fig. 6). In addition, the rise time, fall time and peak-to-peak jitter are respectively evaluated at 889 ps, 556 ps and 666.7 ps? These results indicate that the edge-emitting HBLETs can be used as a high-speed light source for optical communications.

A HBLET-based optical link capable of real-time transmissions of digital video broadcasting-terrestrial (DVB-T) signals over a moderate distance in free space is presented using the proposed optical lens design to facilitate effective light propagation from the optical transmitter to the receiver (referred as a directed line-of-sight optical link). Fig. 7

shows a photograph of the proposed optical wireless transmission system with the edge-emitting HBLET. In the transmitting terminal, the OFDM-based RF signals from the antenna were first demodulated using a commercial DVB-T receiver to generate TV signals. A field programmable gate array (FPGA) based video encoder (Altera CPLD EPM570T144C5N) was then used to obtain a video stream combined with a 50-mA bias current via a high-frequency bias tee and fed to the TO-packaged HBLET. The modulated light from the HBLET will propagate through a moderate distance in free space and eventually return the original TV signals using an optical receiver composed of an optical detector (Pacific AD500-9-400M-TO5), a video decoder (Altera CPLD EPM570T144C5N) and a D/A converter (Texas Instruments TLC5602C) [15]. As shown in Fig. 7, when a directed line-of-sight optical link is established by carefully adjusting the relative positions of two plano-convex lenses so as to maximize the light signals collected by the receiver, real-time TV signals (video only) can be clearly observed on the monitor even when the separation (light coupling efficiency) between the transmitter and the receiver was increased (reduced) from 10 cm (40.6%) to 100 cm (36.5%). In the experiment, the proposed transmission system can still work normally as the transmission distance increases to 2.5 m (the typical distance in indoor optical communications). In such an optical link, the data rate for real-time transmission of digital TV signals is estimated to be about 150 Mbit/s. In contrast to using visible LED transmitters for the realization of optical wireless communications [4–6,15,16], our work indicates that the proposed edge-emitting HBLETs with improved output performance can also be used as an alternative for such communication systems.

4. Conclusions

In summary, the proposed lateral emission design is shown to usefully address the issue associated with light shielding from the metal electrodes of the emitter and base of the HBLETs. Experimental results show HBLETs fabricated with a strip-shaped emitter exhibit an offset voltage of 0.44 V and can provide a 3.7 mA collector current when the base current is set at 9 mA (i.e., $I_C/I_B = 0.41$). In addition to the spontaneous emission of light at $\lambda = 965$ nm, a 12.2% @ $I_E = 60$ mA increase in light output power is achieved as the light was collected laterally to the HBLETs. On the other hand, these edge-emitting HBLETs operated with $V_{BC} = 0$ V and $I_E > 0$ not only exhibit a high modulation bandwidth of 237.5 MHz, but also enable 300 Mbit/s optical data transmission. Finally, real-time transmissions of digital TV signals over a distance of 100 cm in free space are shown to be feasible using a direct line-of-sight optical link with the proposed edge-emitting HBLETs.

Author contribution statement

Chia-Lung Tsai: Conceptualization, Methodology, Validation, Supervision, Writing-
Reviewing and Editing.
Yi-Chen Lu: Investigation, Validation.
Chih-Min Yu: Investigation.
Chia-Yu Yu: Investigation.
Sun-Chien Ko: Resources.
Meng-Chyi Wu: Resources.

Declaration of competing interest

The authors declare that they have no known competing financial interests or personal relationships that could have appeared to influence the work reported in this paper.

Acknowledgements

Financial support was provided by the Ministry of Science and Technology (Taiwan) under Grant MOST 108-2221-E-182-055, MOST 107-2221-E-182-046 and MOST 106-2221-E-182-047, and Chang Gung Memorial Hospital, Linkou (Grant number BMRP 999).

Appendix A. Supplementary data

Supplementary data to this article can be found online at https://doi.org/10.1016/j.optmat.2019.109598.

References

[1] J.H. Reed, J.T. Bernhard, J.M. Park, Spectrum access technologies: the past, the present, and the future, Proc. IEEE 100 (2012) 1676–1684.
[2] M. Ayyash, H. Elgala, A. Khreishah, V. Jungnickel, T. Little, S. Shao, M. Rahaim, D. Schulz, J. Hilt, R. Freund, Coexistence of WiFi and LiFi toward 5G: concepts, opportunities, and challenges, IEEE Commun. Mag. 54 (2016) 64–71.
[3] A. Mansour, R. Mesleh, M. Abaza, New challenges in wireless and free space optical communications, Opt. Lasers Eng. 89 (2017) 95–108.
[4] K. Rae, P.P. Manousiadis, M.S. Islim, L. Yin, J. Carreira, J.J.D. Mckendry, B. Guilhabert, I.D.W. Samuel, G.A. Turnbull, N. Laurand, H. Haas, M.D. Dawson, Transfer-printed micro-LED and polymer-based transceiver for visible light communications, Opt. Express 24 (2018) 31474–31483.
[5] C. Du, X. Huang, C. Jiang, X. Pu, Z. Zhao, L. Jing, W. Hu, Z.L. Wang, Tuning carrier lifetime in InGaN/GaN LEDs via strain compensation for high-speed visible light communication, Sci. Rep. 6 (2016) 37132.
[6] C. Shen, C. Lee, T.K. Ng, S. Nakamura, J.S. Speck, S.P. DenBaars, A.Y. Alyamani, M. M. El-Desouki, B.S. Ooi, High-speed 405-nm superluminescent diode (SLD) with 807-MHz modulation bandwidth, Opt. Express 24 (2016) 20281–20286.
[7] M. Feng, N. Holonyak Jr., R. Chan, Quantum-well-base heterojunction bipolar light-emitting transistor, Appl. Phys. Lett. 84 (2004) 1952–1954.
[8] S.Y. Cheng, Comprehensive study of an InGaP/AlGaAs/GaAs heterojunction bipolar transistor with a continuous conduction-band structure, Semicond. Sci. Technol. 17 (2002) 701–707.
[9] Y.C. Hsieh, E.Y. Chang, S.S. Yeh, C.W. Chang, G.L. Luo, C.Y. Chang, C.T. Lee, Optimization of the growth of the InGaP etch-stop layer by MOVPE for InGaP/GaAs HBT device application, J. Cryst. Growth 289 (2006) 96–101.
[10] A. Kapila, V. Malhotra, L.H. Camnitz, K.L. Seaward, D. Mars, Passivation of GaAs surfaces and AlGaAs/GaAs heterojunction bipolar transistors using sulfide solutions and SiN_x overlayer, J. Vac. Sci. Technol. B 13 (1995) 10–14.
[11] W. Liu, Extrinsic base surface recombination current in GaInP/GaAs heterojunction bipolar transistors with near-unity ideality factor, Jpn. J. Appl. Phys. 32 (1993) L713–L715.
[12] P.M. Asbeck, R.J. Welty, C.W. Tu, H.P. Xin, R.E. Welser, Heterojunction bipolar transistors implemented with GaInNAs materials, Semicond. Sci. Technol. 17 (2002) 898–906.
[13] H.C. Lin, Diode operation of a transistor in functional blocks, IEEE Trans. Electron Devices 10 (1963) 189–194.
[14] L. Wang, N.M. Haegel, J.R. Lowney, Band-to-band photoluminescence and luminescence excitation in extremely heavily carbon-doped epitaxial GaAs, Phys. Rev. B 49 (1994) 10976–10985.
[15] C.L. Tsai, Y.J. Chen, Real-time optical wireless transmissions of digital TV signals using white InGaN LEDs grown with an asymmetric quantum barrier, Opt. Express 23 (2015) 28059–28066.
[16] X. Gao, D. Bai, W. Cai, Y. Xu, J. Yuan, Y. Yang, G. Zhu, X. Cao, H. Zhu, Y. Wang, Membrane-type photonic integration of InGaN/GaN multiple-quantum-well diodes and waveguide, Opt. Mater. 64 (2017) 160–165.
[17] C.H. Wu, G. Walter, H.W. Then, M. Feng, N. Holonyak Jr., 4-GHz modulation bandwidth of integrated 2×2 LED array, IEEE Photonics Technol. Lett. 21 (2009) 1834–1836.
[18] W. Huo, S. Liang, C. Zhang, S. Tan, L. Han, H. Xie, H. Zhu, W. Wang, Fabrication and characterization of deep ridge InGaAsP/InP light emitting transistors, Opt. Express 22 (2014) 1806–1814.